Journal of Renewable Materials

Tech Science Press

DOI: 10.32604/jrm.2023.025431

ARTICLE

The Adsorption of Pb(II) Using Silica Gel Synthesized from Chemical Bottle Waste: Optimization Using Box-Behnken Design

Yatim Lailun Ni'mah*, Nabila Eka Yuningsih and Suprapto Suprapto

Department of Chemistry, Faculty of Science and Data Analytics, Institut Teknologi Sepuluh Nopember, Surabaya, Indonesia

*Corresponding Author: Yatim Lailun Ni'mah. Email: yatimnikmah@gmail.com

Received: 12 July 2022 Accepted: 28 September 2022

ABSTRACT

The adsorption of Pb(II) on silica gel synthesized from chemical glass bottle waste has been studied. The effect of independent variables (adsorbent dose, initial concentration of Pb(II), contact time, and pH) on the Pb(II) removal from water was evaluated and optimized using the Response Surface Methodology (RSM). Under optimized conditions (adsorbent dose: 20 mg; contact time: 30 min; initial Pb(II) concentration: 120 $mg.L^{-1}$; and pH: 8), the removal of Pb(II) was 99.77%. The adsorption equilibrium data obtained from the batch experiment were investigated using different isotherm models. The Langmuir isotherm model fits the experimental data. This shows that the surface of the silica gel synthesized from chemical bottles waste was covered by a Pb(II) monolayer. XRF analysis showed that the synthesized silica gel had a SiO_2 content of 75.63%. Amorphous silica was observed from XRD analysis. SEM-EDX characterization showed that Pb was adsorbed on the silica gel surface. SEM analysis showed that silica gel has irregular particles with a surface area of 297.08 $m^2.g^{-1}$ with a pore radius of 15.74 nm calculated from BET analysis.

KEYWORDS

Chemical bottle waste; silica gel; adsorption; box-behnken design; response surface methodology

1 Introduction

Europe and Central Asia generated 31.36 million tonnes of glass waste in 2016 [1]. Glass waste is inorganic waste and is classified as hazardous waste. Chemical bottle waste is one the hazardous wastes that cannot be decomposed naturally and requires special handling [2]. The utilization of chemical glass bottle waste depends on its chemical composition. In general, chemical bottled glass waste contains silica (65%–75%), sodium oxide (12%–15%), calcium oxide (6%–12%) [3], and several other minor constituents. The high silica content in chemical bottle glass waste makes it prospective to be used as a precursor in the synthesis of silica gel [4]. Several studies have shown that silica gel has high porosity, small pore size, and large surface area, so it can be used as an adsorbent [5,6].

Several methods have been applied for the synthesis of silica gel, including the sol-gel method [4,5,7], heating [8], hydrothermal [3] reflux [9], and composites [10–12]. The sol-gel method has advantages such as producing a homogeneous product, low processing temperature, and can produce nanoparticles. In this study, silica gel was synthesized from alkaline fusion and the sol-gel method. Silica extraction was carried out using

the alkaline fusion method to convert glass bottle waste into sodium silicate and then convert it into silica gel using the sol-gel method.

Heavy metal pollution in waste generated from industrial processes, such as metal plating, metal mining, leather tanning, Chlor-alkali, mineral smelting, microplastics [13], and the battery industry [14], is a serious environmental problem. Due to their high solubility in aquatic environments, heavy metals can be ingested by living organisms. Once they enter the food chain, large amounts of heavy metals can accumulate in the human body. Lead (Pb) contamination is of particular concern because of its toxicity and its widespread presence in the environment. Lead is one of the most dangerous heavy metals. Lead is a systemic poison that causes anemia, kidney dysfunction, and brain tissue damage and is even fatal in extreme poisoning situations. The presence of lead in the environment can pose long-term health risks to humans and ecosystems. According to the World Health Organization (WHO), the maximum allowable limit (MPL) for lead in drinking water is 0.05 $mg.L^{-1}$. The allowable limit ($mg.L^{-1}$) for Pb(II) in effluents set by the Environmental Protection Agency (EPA) is 0.05 $mg.L^{-1}$ [15,16]. In industrial effluents, the lead ion concentration can reach 200–500 $mg.L^{-1}$. The lead ion concentration from wastewater must be reduced to 0.05–0.10 $mg.L^{-1}$ before being allowed to discharge into waterways or sewage systems [17,18].

Several methods have been used to reduce lead levels in wastewater, namely coagulation, flocculation [15], biodegradation [17,19], remediation [16,20] adsorption [12,21] and coagulation [22]. The adsorption method is superior to other methods in terms of cost, process, and chemical use [6,23]. Rahman et al. [6] research obtain a Pb(II) removal of 99.78% using 0.2 g of adsorbent in 20 mL of 50 $mg.L^{-1}$ lead solution at pH 6. Optimization was carried out using Box-Behnken Design with 4 factors, namely adsorbent mass, contact time, initial concentration of Pb(II), and pH. Each variable was optimized at 3 levels.

The application of Design of Experiment (DoE) in optimization provides several advantages, namely fewer experiments, less reagent consumption, and less laboratory work [24]. The use of the classical approach for optimization is considered less economical and practical because it requires more experiments to run. Response Surface Methodology (RSM) is a statistical tool for estimating the optimal response as a function of more than one input factor. The optimization is presented in a graph using polynomial regression [24,25]. Box-Behnken Design (BBD) was used to optimize the input variables that affect the removal of Pb(II). The input variables that were optimized in this study were the adsorbent dose, contact time, initial concentration of Pb(II), and pH. The correlation between input factors and experimental results was visualized using the response surface (RSM) methodology [26].

2 Experimental

2.1 Material Preparation

The materials used in this research were chemical glass bottle waste and sodium hydroxide (98%, Merck). Chemical glass bottle waste was obtained from the ITS Chemistry Department Laboratory, Surabaya, Indonesia. Glass bottles were initially rinsed, dried, and crushed using a jaw crusher to obtain a coarse powder. Coarse glass powder was ground using a Disc Mill to obtain a fine glass powder. Milling was carried out for 2 min at a rate of 2 rpm. The glass powder was sieved to obtain a powder with a particle size of 45–53 μm (200–230 mesh).

2.2 The Optimization of Pb(II) Adsorption

Response Surface Methodology (RSM)-Box-Behnken Design (BBD) was applied to optimize Pb(II) adsorption. The python package was used to generate BBD input, regression analysis, and 3D surface response plots for Pb(II) adsorption [6]. In optimizing Pb(II) adsorption, four independent factors were selected, namely adsorbent dose (x1), initial Pb(II) concentration (x2), contact time (x3), and pH (x4). Each factor was investigated at three levels (high (+1), center point (0), and low (1)), as shown in Table 1.

Table 1: Box-behnken design for the adsorption of Pb(II)

Variables	Levels		
	−1	0	1
Adsorbent dose (mg, x1)	15	20	25
Initial concentration (mg · L^{-1}, x2)	50	100	150
Contact time (min, x3)	10	20	30
pH (x4)	4	7	10

The BBD design produces 27 combinations of factors and levels to optimize Pb(II) adsorption. RSM was applied to optimize the factors associated with Pb(II) removal and the interaction between response and factors.

2.3 The Synthesis of Silica Gel from Chemical Glass Waste

The synthesis of silica gel from glass bottle waste was carried out by mixing glass powder and sodium hydroxide. Synthesis was carried out with a ratio of silica and sodium hydroxide 2:6 (w/w). The mixture was heated at 800°C for 4 h. The resulting sodium silicate was dissolved in 50 ml of boiling water. The sodium silicate solution was filtered to remove impurities. Hydrochloric acid 3 M was added to the sodium silicate dropwise and stirred using a magnetic stirrer at a rate of 450 rpm until a white gel was formed. The gel was allowed to stand for 18 h, after that it was filtered and dried in an oven at 80°C for 12 h to form silica gel.

2.4 The Adsorption of Pb(II)

The adsorption of Pb(II) on silica gel was optimized by varied adsorbent masses (15, 20, and 25 mg), the initial Pb(II) concentration (50, 100, 150 mg.L^{-1}), contact time (10, 20, and 30 min), and pH (4, 7, 10) using 20 ml Pb(II) solution. The Pb(II) removal was calculated using Eq. (1)

$$\text{Removal } (\%) = 100\left(\frac{Co - Ce}{Co}\right) \tag{1}$$

where Co and Ce were the Pb(II) initial and equilibrium concentrations in the solution (mg · L^{-1}), respectively. The initial (Co) and the equilibrium (Ce) concentrations were determined from the calibration curve of the Pb(II) standard solution.

2.5 Characterization

X-Ray Diffractometer (Rigaku SmartLab®) was used to determine the structure of glass powder and silica gel. X-Ray Fluorescence (Rigaku ZSX Primus IV) was used to determine the composition of glass powder and silica gel. A surface Area Analyzer (Quantachrome Autosorb IQ) was used to determine the surface area and pore size of silica gel. Scanning Electron Microscope-Energy Dispersive X-Ray (Bruker EVO MA 10) was employed to determine the morphology and surface composition of silica gel. Atomic Absorption Spectroscopy (iCE 3000 Series) was used to determine the concentration of Pb(II).

3 Results and Discussion

3.1 Optimization of Pb(II) Adsorption

Experiments with 27 runs were carried out to optimize the adsorbent dose, initial concentration of Pb(II), contact time, and pH on Pb(II) removal using silica gel as adsorbent. The RSM curve obtained from the experiment was shown in Fig. 1.

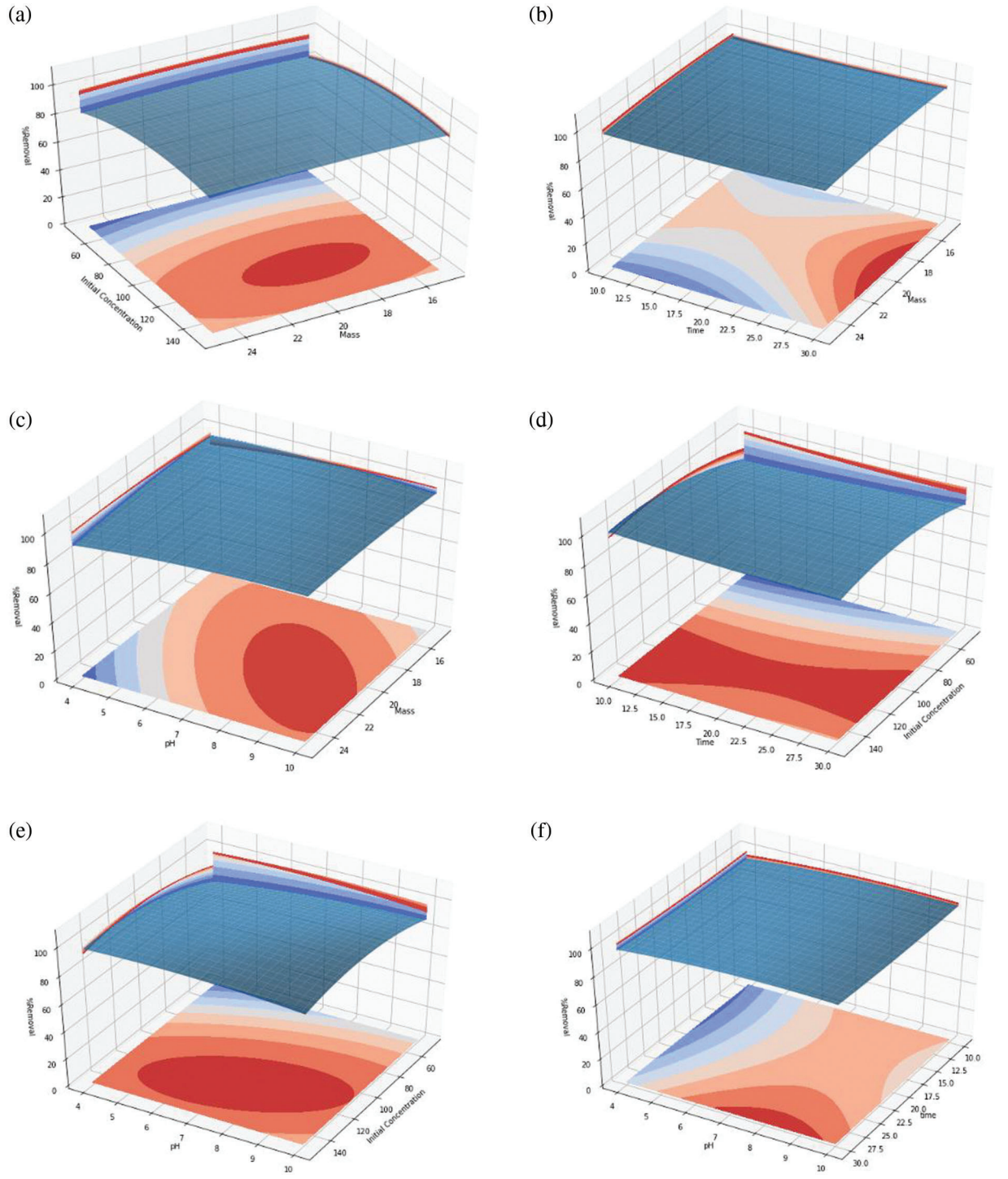

Figure 1: The RSM plot of Pb(II) removal as the function of adsorbent mass, Pb(II) initial concentration, contact time, and pH

Multiple regression analysis of experimental data gives a correlation coefficient (r^2) of 0.827 with the slope and intercept as described in Eq. (2). This correlation coefficient (r^2) indicates that the input variable has a good correlation with the output variable (Pb(II) removal).

$$\begin{aligned} Y = {} & 13.5582 + 1.376733x_1 + 0.993547x_2 + 0.156783x_3 + 3.552074x_4 - 0.068358x_1^2 \\ & + 0.000390x_1x_2 + 0.005310x_1x_3 + 0.156350x_1x_4 - 0.005697x_2x_3 - 0.023272x_2x_4 \\ & - 0.005167x_3x_4 - 0.003003x_2^2 + 0.011077x_3^2 - 0.258954x_4^2 \end{aligned} \quad (2)$$

where x_1, x_2, x_3, and x_4 were adsorbent dose, Pb(II) initial concentration, contact time, and pH, respectively.

The relationship between input variables and Pb(II) removal was studied using the response surface curve. A three-dimensional response surface curve was obtained by plotting the response (% removal) on the Z-axis to the two input variables while other variables were kept at the "0" level [26]. Based on the response surface curve, Pb^{2+} removal was increased in the mass of the adsorbent from 18 to 22 mg with increasing concentration from 110 to 130 ppm, as shown in Fig. 1a. The Pb(II) removal increased as the adsorbent mass increased from 17 to 22 mg with a contact time of 30 min, as shown in Fig. 1b. Pb(II) removal increased as adsorbent mass and pH increased. The optimum adsorbent masses were from 18 to 22 mg with a pH of 7 to 9, as shown in Fig. 1c. Pb(II) removal increased as contact time and concentration increased. The optimum contact times were from 10 to 30 min at a concentration of 90 to 130 ppm, as shown in Fig. 1d. The increase of initial Pb(II) concentration and pH increases the Pb(II) removal. The optimum removal was obtained at concentrations of 100 to 130 ppm and a pH of 5 to 10, as shown in Fig. 1e. The optimum Pb(II) removal was achieved at a contact time of 30 min and pH from 7 to 9, as shown in Fig. 1f.

The optimum Pb(II) removal was obtained at the adsorbent mass of 20 mg, contact time of 30 min, Pb(II) initial concentration of 120 ppm, and pH 8. Based on Eq. (2) the optimum Pb(II) removal obtained was 99.77%. The Pb(II) removal in this research was higher than in Rahman et al. [6]. The utilization of glass bottle waste into silica adsorbent can reduce waste and has good environmental impacts. The *p*-value from the regression analysis was 0.00946. It indicated that the independent variables have a significant effect on Pb(II) removal [24].

3.2 Characterization

3.2.1 N_2 Adsorption-Desorption Analysis

The determination of the silica gel surface area and pore size was carried out by nitrogen adsorption-desorption using the BET (Brunauer-Emmet-Teller) method. The determination of pore size was carried out using the BJH method. The nitrogen adsorption curve was shown in Fig. 3a. Based on Fig. 3a, the Pb(II) adsorption on silica gel follows type IV isotherm. This indicates that the synthesized silica gel tends to have a mesoporous structure. This type of isotherm was associated with capillary condensation that occurs in the mesoporous structure and has a limited absorption rate in the high P/P^0 region. The loop type was H3 which indicates the presence of an ink bottle-shaped pore. The surface area obtained was 297.08 $m^2 \cdot g^{-1}$. The pore size distribution was shown in Fig. 2b. The pore radius obtained was 15.74 nm.

3.2.2 X-Ray Fluorescence (XRF) Analysis

The XRF analysis of glass powder and silica gel was shown in Table 2. Based on the XRF data, the glass powder has SiO_2 of 63.74%, Na_2O of 12.88%, and CaO of 10.95%. These results were in accordance with the research conducted by Owoeye et al. [4]. Thus, glass bottle waste has the potential to be extracted as a precursor for the synthesis of silica gel that was prepared as a Pb(II) adsorbent.

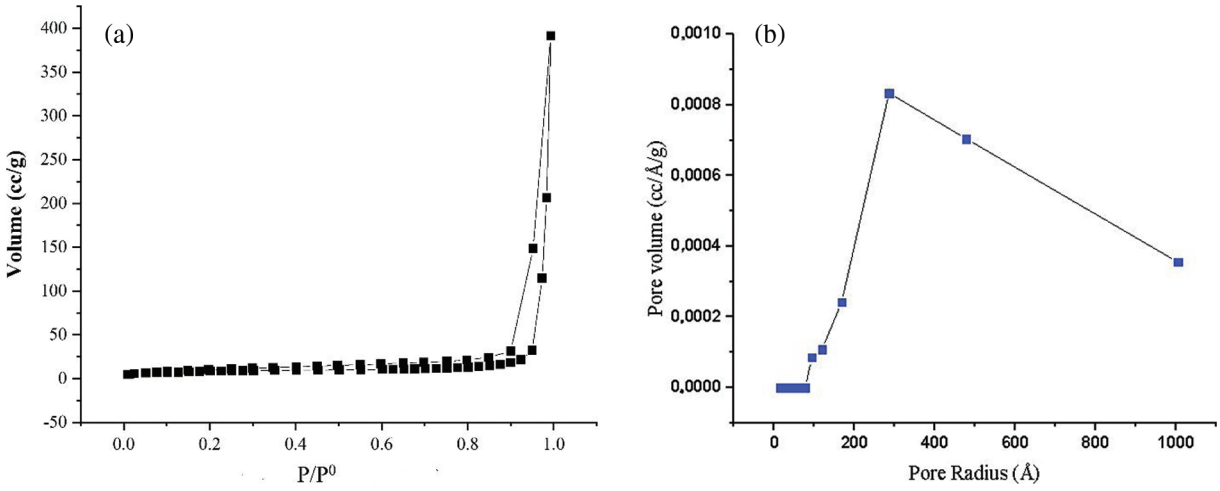

Figure 2: (a) Nitrogen adsorption-desorption on silica gel and (b) BJH curve of silica gel

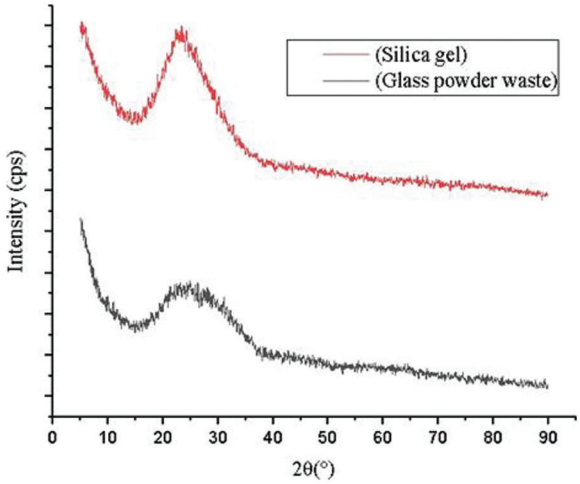

Figure 3: Diffractogram of glass powder waste and silica gel

Table 2: XRF characterization

Glass waste		Silica gel	
Compounds	% w/w	Compounds	% w/w
Al_2O_3	2.04	Al_2O_3	8.39
SiO_2	63.74	SiO_2	75.63
B_2O_3	2.30	MgO	0.12
Na_2O	12.88	CO_2	5.66
Cl	0.02	Na_2O	8.19
K_2O	0.75	Cl	0.71
CaO	10.95	K_2O	0.27

(Continued)

Table 2 (continued)

Glass waste		Silica gel	
Compounds	% w/w	Compounds	% w/w
TiO_2	0.13	CaO	0.09
Cr_2O_3	0.04	Cr_2O_3	0.28
MnO	0.02	MnO	0.06
Fe_2O_3	0.62	Fe_2O_3	0.54
NiO	0.00	NiO	0.03
CuO	0.01	CuO	0.01
Rb_2O	0.00		
SrO	0.03		
ZrO_2	0.01		
BaO	0.07		
MgO	1.91		
CO_2	3.53		

Based on the XRF analysis, the silica or SiO_2 content in the synthesized silica gel was 75.63%. The other major constituents were Na_2O (8.19%) and Al_2O_3 (8.39%). Table 2 shows that the purity of silica increased after the extraction. Thus, the extraction process removes some impurities from the silica gel.

3.2.3 X-Ray Diffraction Characterization

The XRD characterization of initial glass powder and silica gel shows a broad peak of silica at 2θ 22–27°. XRD spectra indicated that glass powder and silica gel have an amorphous phase. Increasing the diffractogram peak intensity of the silica gel indicates that the SiO_2 in silica gel has higher purity than in glass powder. Based on Owoeye et al. [4], amorphous silica was identified as a soluble form of silica and suitable for heavy metal adsorbent.

3.2.4 SEM-EDX Characterization

Silica gel surface morphology, as well as its composition, before (Fig. 4a) and after (Fig. 4b) adsorption were characterized using SEM-EDX. Fig. 4a shows silica gel micrographs synthesized from chemical bottle waste at 500× magnification. The silica gel particles were irregular with a spherical shape. This was similar to the previous study [3,27]. Fig. 4b shows that the synthesized silica gel contains Si, Pb, C, and O as major constituents with other minor constituents at 500× magnification. Table 3 shows that Pb was present on the surface of the adsorbent after the adsorption process.

3.3 Adsorption Isotherm

The adsorption isotherm of Pb(II) adsorption on silica gel was studied to investigate the adsorption mechanism. The adsorption isotherm describes the concentration of Pb(II) adsorbed in the unit mass of the solid at a constant temperature at equilibrium conditions [28,29]. The adsorption can be physical adsorption caused by van der Waals forces or chemical adsorption caused by chemical bonds such as covalent or ionic bonds. The physical adsorption is relatively weak and reversible with the heat of

adsorption in only a few kcal/mol. The Langmuir isotherm is a model of physical adsorption. In chemical adsorption, the interaction between molecules on the surface of the adsorbent is a chemical bonding, so the adsorption is irreversible. The heat of adsorption is relatively high, and the adsorption is usually monomolecular. Brunauer-Emmett-Teller, or BET isotherms, is an example of a chemical adsorption model. The type of adsorption can be determined by constructing an adsorption isotherm to determine whether it is physical adsorption, chemical adsorption, or both. The model goodness of fit was determined from the value of the determination coefficient (r^2) [30]. The adsorption isotherm of Pb(II) on silica gel was shown in Fig. 5. The regression analysis was summarized in Table 4. The Pb(II) adsorption on silica gel was fitted well to the Langmuir isotherm model based on its determination coefficient (r^2), 0.9345, as shown in Fig. 5a. The isotherm model indicated that physical adsorption with a monolayer surface was formed [31]. The adsorption occurred due to the attraction of Pb(II) to the surface of the silica gel adsorbent by Van der Waals forces or hydrogen bonds. The silica gel adsorbent has a homogeneous adsorption site distribution, and its adsorption process was monolayer adsorption [32].

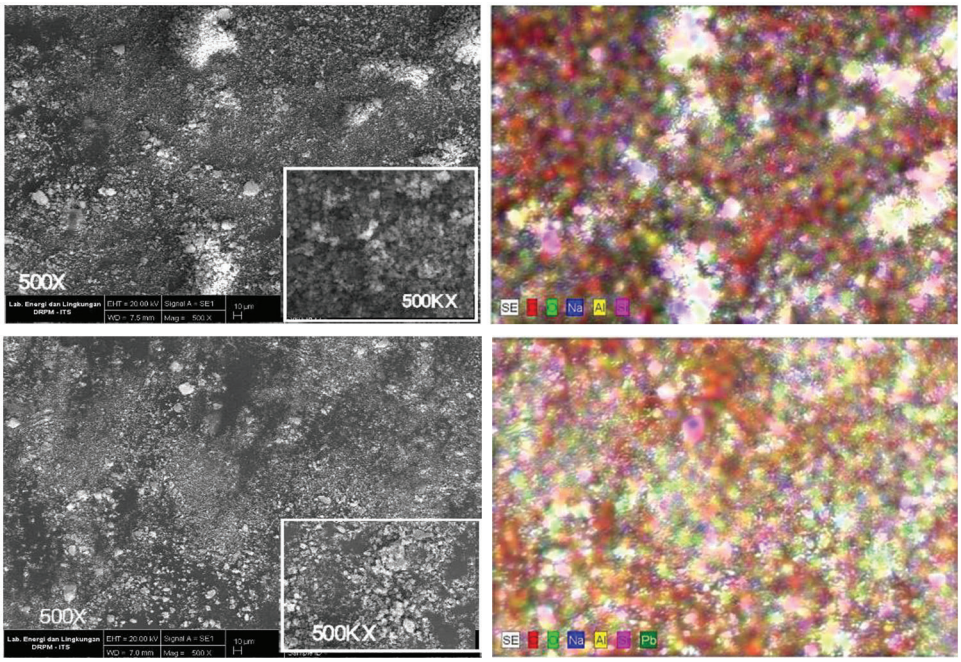

Figure 4: The silica gel morphology (a) before and (b) after adsorption

Table 3: The silica gel surface composition before and after adsorption

Samples	% w/w					
	O	C	Si	Na	Al	Pb
Silica gel before adsorption	49.87	45.71	2.70	1.20	0.52	-
Silica gel after adsorption	27.71	39.75	5.56	1.04	0.98	24.96

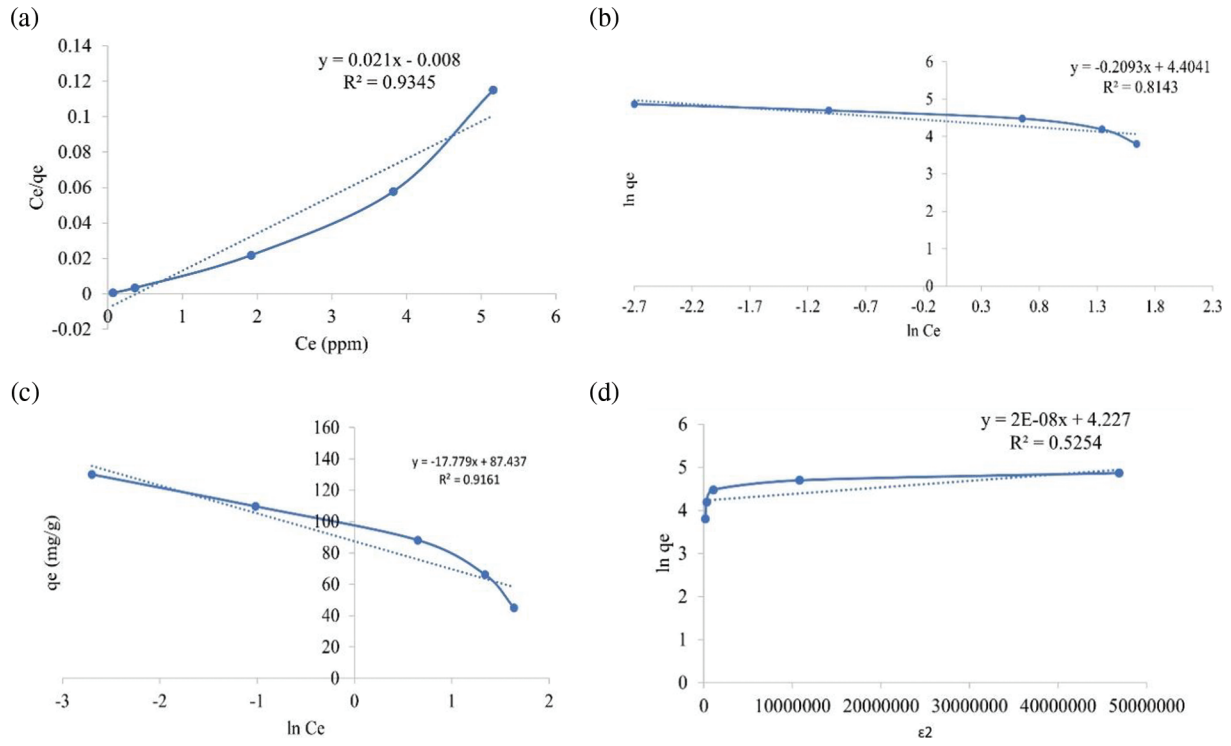

Figure 5: The regression curve of experimental data based on (a) Langmuir, (b) Freundlich, (c) Temkin and (d) Dubinin-Radushkevich isotherm

Table 4: Isotherm parameters from regression analysis

Isotherm parameters		
Langmuir	qm ($mg.g^{-1)}$	47.619
	K_L ($L.mg^{-1}$)	−2.625
	R^2	0.9350
Freundlich	n	−4.778
	K_f ($mg.g^{-1}$)	81.786
	R^2	0.8143
Temkin	B_T ($J.mol^{-1}$)	87.473
	K_T ($L.mg^{-1}$)	0.816
	R^2	0.9161
Dubinin-Radushkevich	qm ($mg.g^{-1}$)	1.000
	β ($mol^2.J^{-2}$)	−4.227
	E ($kJ.mol^{-1}$)	0.354
	R^2	0.5254

4 Conclusion

Pb(II) removal of 99.77% has been achieved by adsorption using silica gel synthesized from chemical glass bottle waste. The adsorption followed the Langmuir isotherm model. The synthesized silica gel surface area was 297.08 $m^2 \cdot g^{-1}$ with a pore radius of 15.74 nm. The success of the Pb(II) adsorption on silica gel synthesized from chemical bottle glass waste using the RSM method shows its feasibility to be used for the adsorption of other heavy metals.

Funding Statement: The authors received no specific funding for this study.

Conflicts of Interest: The authors declare that they have no conflicts of interest to report regarding the present study.

References

1. Alkatiri, D. S. F., Insani, A. M., Marjuki, E. I., Fithriyah, N. H. (2017). Pembuatan Gel silika dari limbah kaca dengan bantuan ultrasound bath dan microwave. *Prosiding Seminar Nasional Sains dan Teknologi*, pp. 1–5. Jakarta, Indonesia.
2. Kamseu, E., Moungam, B., Cannio, M., Billong, N., Chaysuwan, D. et al. (2017). Substitution of sodium silicate with rice husk ash-NaOH solution in metakaolin based geopolymer cement concerning reduction in global warming. *Journal of Cleaner Production, 142,* 3050–3060. https://doi.org/10.1016/j.jclepro.2016.10.164
3. Owoeye, S. S., Abegunde, S. M., Oji, B. (2021). Effects of process variable on synthesis and characterization of amorphous silica nanoparticles using sodium silicate solutions as precursor by sol–gel method. *Nano-Structures and Nano-Objects, 25,* 100625. https://doi.org/10.1016/j.nanoso.2020.100625
4. Owoeye, S. S., Jegede, F. I., Borisade, S. G. (2020). Preparation and characterization of nano-sized silica xerogel particles using sodium silicate solution extracted from waste container glasses. *Materials Chemistry and Physics, 248,* 122915. https://doi.org/10.1016/j.matchemphys.2020.122915
5. Sudjarwo, W. A. A., Bee, M. M. F. (2017). Synthesis of silica gel from waste glass bottles and its application for the reduction of free fatty acid (FFA) on waste cooking oil. *AIP Conference Proceedings, 1855(1),* 020019. https://doi.org/10.1063/1.4985464
6. Rahman, N., Nasir, M., Varshney, P., Al-Enizi, A. M., Ubaidillah, M. et al. (2021). Efficient removal of Pb(II) from water using silica gel functionalized with thiosalicylic acid: Response surface methodology for optimization. *Journal of King Saud University-Science, 33(1),* 101232. https://doi.org/10.1016/j.jksus.2020.101232
7. Biradar, A. I., Sarvalkar, P. D., Teli, S. B., Pawar, C. A., Patil, P. S. et al. (2021). Photocatalytic degradation of dyes using one-step synthesized silica nanoparticles. *Materials Today: Proceedings, 43(4),* 2832–2838.
8. Ramadani, K. (2018). Sintesis dan karakterisasi silika gel dari limbah kaca untuk menurunkan kesadahan air. *Jurnal Saintifik, 4(2),* 179–185. https://doi.org/10.31605/saintifik.v4i2.183
9. Asadi, Z., Norouzbeigi, R. (2018). Synthesis of colloidal nanosilica from waste glass powder as a low cost precursor. *Ceramics International, 44(18),* 22692–22697. https://doi.org/10.1016/j.ceramint.2018.09.050
10. Khadra, M. R. A., Mohamed, A. S., El-Sherbeeny, A. M., Elmeligy, M. A. (2020). Enhanced photocatalytic degradation of acephate pesticide over MCM-41/Co_3O_4 nanocomposite synthesized from rice husk silica gel and peach leaves. *Journal of Hazardous Materials, 389,* 122129. https://doi.org/10.1016/j.jhazmat.2020.122129
11. Kalu, O. I., Subramanian, B., MacLean, B. J., Saha, G. C. (2019). A novel approach to the sol-gel synthesis of titanium dioxide-coated SBA-16 type silica mesoporous microspheres for water purification. *Materialia, 5,* 100237. https://doi.org/10.1016/j.mtla.2019.100237
12. Younes, M. M., El-Sharkawy, I. I., Kabeel, A. E., Uddin, K., Miyazaki, T. et al. (2020). Characterization of silica gel-based composites for adsorption cooling applications. *International Journal of Refrigeration, 118,* 345–353. https://doi.org/10.1016/j.ijrefrig.2020.04.002
13. Khalid, N., Aqeel, M., Noman, A., Khan, S. M., Akhter, N. (2021). Interactions and effects of microplastics with heavy metals in aquatic and terrestrial environments. *Environmental Pollution, 290,* 118104. https://doi.org/10.1016/j.envpol.2021.118104

14. Bilge, S., Karadurmus, L., Sınağ, A., Ozkan, S. A. (2021). Green synthesis and characterization of carbon-based materials for sensitive detection of heavy metal ions. *TrAC Trends in Analytical Chemistry, 145,* 116473. https://doi.org/10.1016/j.trac.2021.116473
15. Hargreaves, A. J., Whelan, P. V. J., Alibardi, L., Constantino, C., Dotro, G. et al. (2018). Impacts of coagulation-flocculation treatment on the size distribution and bioavailability of trace metals (Cu, Pb, Ni, Zn) in Municipal Wastewater. *Water Research, 128,* 120–128.
16. Xue, Z. F., Cheng, W. C., Wang, L., Hu, W. (2022). Effects of bacterial inoculation and calcium source on microbial-induced carbonate precipitation for lead remediation. *Journal of Hazardous Materials, 426,* 128090. https://doi.org/10.1016/j.jhazmat.2021.128090
17. Lin, W., Huang, Z., Li, X., Liu, M., Cheng, Y. (2016). Bio-remediation of acephate–Pb(II) compound contaminants by bacillus subtilis FZUL-33. *Journal of Environmental Science, 45,* 94–99. https://doi.org/10.1016/j.jes.2015.12.010
18. Zhang, D., Yang, S., Ma, Q., Sun, J., Cheng, H. et al. (2020). Simultaneous multi-elemental speciation of as, Hg and Pb by inductively coupled plasma mass spectrometry interfaced with high-performance liquid chromatography. *Food Chemistry, 313,* 126119. https://doi.org/10.1016/j.foodchem.2019.126119
19. Malaviya, P., Singh, A. (2011). Physicochemical technologies for remediation of chromium-containing waters and wastewaters. *Critical Reviews in Environmental Science and Technology, 4(12),* 1111–1172. https://doi.org/10.1080/10643380903392817
20. Tee, W. T., Loh, N. Y. L., Hiew, B. Y. Z., Hanson, S., Gopakumar, S. T. et al. (2022). Effective remediation of lead (II) wastewater by *Parkia speciosa* pod biosorption: Box-behnken design optimisation and adsorption performance evaluation. *Biochemical Engineering Journal, 187,* 108629. https://doi.org/10.1016/j.bej.2022.108629
21. Zeng, S., Wang, J., Li, P., Dong, H., Wang, H. et al. (2019). Efficient adsorption of ammonia by incorporation of metal ionic liquids into silica gels as mesoporous composites. *Chemical Engineering Journal, 370,* 81–88. https://doi.org/10.1016/j.cej.2019.03.180
22. Meng, X., Khoso, S. A., Jiang, F., Zhang, Y., Yue, T. et al. (2020). Removal of chemical oxygen demand and ammonia nitrogen from lead smelting wastewater with high salts content using electrochemical oxidation combined with coagulation-flocculation treatment. *Separation and Purification Technology, 235,* 116233. https://doi.org/10.1016/j.seppur.2019.116233
23. Ifijen, I. H., Itua, A. B., Maliki, M., Ize-Imayu, C. O., Omorogbe, S. O. et al. (2020). The removal of nickel and lead ions from aqueous solutions using green synthesized silica microparticles. *Heliyon, 6(9),* e04907. https://doi.org/10.1016/j.heliyon.2020.e04907
24. Rahbar, N., Ramezani, Z., Ghanavati, J. (2016). CuO-nanoparticles modified carbon paste electrode for square wave voltammetric determination of lidocaine: Comparing classical and box–behnken optimization methodologies. *Chinese Chemical Letters, 27(6),* 837–842. https://doi.org/10.1016/j.cclet.2016.04.017
25. Khair, A., Putri, H. A., Suprapto, S., Ni'mah, Y. L. (2021). The optimization of Sumbawa manganese ore beneficiation using response surface method (RSM). *AIP Conference Proceeding, 2349(1),* 020050. https://doi.org/10.1063/5.0051614
26. Ding, H., Li, J., Gao, Y., Zao, D., Shi, D. et al. (2015). Preparation of silica nanoparticles from waste silicon sludge. *Powder Technology, 284,* 231–236. https://doi.org/10.1016/j.powtec.2015.06.063
27. Imoisili, P. E., Ukoba, K. O., Jen, T. C. (2020). Green technology extraction and characterisation of silica nanoparticles from palm kernel shell ash via sol-gel. *Journal of Materials Research and Technology, 9(1),* 307–313. https://doi.org/10.1016/j.jmrt.2019.10.059
28. Teong, C. Q., Setiabudi, H. D., El-Arish, N. A. S., Bahari, M. B., Teh, L. P. (2021). Vatica rassak wood waste-derived activated carbon for effective Pb(II) adsorption: Kinetic, isotherm, and reusability studies. *Materials Today Proceedings, 42(1),* 165–171. https://doi.org/10.1016/j.matpr.2020.11.270
29. Mehdinia, A., Heydari, S., Jabbari, A. (2020). Synthesis and characterization of reduced graphene oxide-Fe_3O_4@polydopamine and application for adsorption of lead ions: Isotherm and kinetic studies. *Materials Chemistry and Physics, 239,* 121964. https://doi.org/10.1016/j.matchemphys.2019.121964

30. Onder, A., Ilgin, P., Ozay, H., Ozay, O. (2020). Removal of dye from aqueous medium with pH sensitive poly[(2-(acryloyloxy)ethyl]trimethylammonium chloride-co-1-vinyl-2-pyrrolidone] cationic hydrogel. *Journal of Environmental Chemical Engineering, 8(5),* 104436. https://doi.org/10.1016/j.jece.2020.104436
31. Wang, H., Wang, S., Wang, S., Tang, J., Chen, Y. et al. (2022). Adenosine-functionalized UiO-66-NH_2 to efficiently remove Pb(II) and Cr(VI) from aqueous solution: Thermodynamics, kinetics, and isothermal adsorption. *Journal of Hazardous Materials, 425,* 127771. https://doi.org/10.1016/j.jhazmat.2021.127771
32. Fang, Y., Ren, G., Wang, C., Li, M., Pang, X. et al. (2022). Adsorption and reutilization of Pb(II) based on acid-resistant metal-organic gel. *Separation and Purification Technology, 295,* 121253. https://doi.org/10.1016/j.seppur.2022.121253